

# Supramolecular Hybrids of Chiral Waugh Polyoxometalate with Cyclodextrins

Zhen-Qin Qi, Ming-Yue Wang, Jia-Chi Shen, You-Zhao Lan, Zhan-Guo Jiang\*, Cai-Hong Zhan\*

## Table of Contents

S1. Materials .....	2
S2. General Experimental Section.....	2
Powder X-ray Diffraction (PXRD).....	2
Fourier Transform Infrared Spectroscopy (FTIR).....	2
Elemental Analyses (EA).....	2
Thermogravimetric Analyses (TGA) .....	2
Nuclear Magnetic Resonance spectra (NMR) .....	2
Single-crystal X-ray diffraction (SCXRD) .....	3
S3. Synthesis and Experimental Section .....	4
The synthesis of 1: .....	4
The synthesis of 2: .....	4
S4. Crystal data and structure refinement.....	5
S5. Additional structural figures .....	6
S6. <sup>1</sup> H NMR spectra .....	9
S7. Fourier Transform Infrared Spectroscopy.....	11
S8. Powder X-ray diffraction (PXRD) .....	12
S9. Thermogravimetric analyses (TGA) .....	14
S11. Enantiomers of {MnMo <sub>9</sub> } in 1 and 2.....	16
S12. Isothermal Titration Calorimetry (ITC) .....	16
S13. Circular dichroism (CD) .....	18

## **S1. Materials**

All starting materials and reagents were purchased from commercial suppliers and used without further purification.  $\beta$ -Cyclodextrins (98%) and  $\gamma$ -Cyclodextrins (98%) were purchased from Aladdin.  $(\text{NH}_4)_6[\text{MnMo}_9\text{O}_{32}] \cdot 8\text{H}_2\text{O}$  is synthesized by reference (Journal of Hebei Normal University (Natural Science Edition), 2002, 22: 19.).

## **S2. General Experimental Section**

### **Powder X-ray Diffraction (PXRD)**

Powder XRD patterns were obtained using a Bruker D8 Advance X-ray diffractometer with ( $\lambda$  (CuK $\alpha$ ) = 1.5405 Å) radiation.

### **Fourier Transform Infrared Spectroscopy (FTIR)**

The materials were recorded on KBr disk using a Nicolet NEXUS 670 spectrometer between 400 and 4000  $\text{cm}^{-1}$ .

### **Elemental Analyses (EA)**

C H N S microanalyses were performed on a Perkin-Elmer 240C elemental analyser, and EDS analyses were carried out on a Zeiss geminiseM 300 field emission scanning electron microscope.

### **Thermogravimetric Analyses (TGA)**

They were carried out on a TA Instruments STA499 F5 thermobalance with a 100  $\text{mL} \cdot \text{min}^{-1}$  flow of nitrogen; the temperature was ramped from 20 °C to 800 °C at a rate of 10 °C  $\cdot \text{min}^{-1}$ .

### **Nuclear Magnetic Resonance spectra (NMR)**

The NMR spectra were recorded on a Bruker Advance III 600 MHz instrument at room temperature, using 5 mm tubes. Generally,  $\{\text{MnMo}_9\}$  sample and CDs were respectively dissolved in  $\text{D}_2\text{O}$ .

## Single-crystal X-ray diffraction (SCXRD)

A suitable crystal of **1** and **2** were mounted in a Hampton cryoloop with Paratone® N oil cryoprotectant. Intensity data collections were carried out at  $T = 160(2)$  K with a Bruker D8 VENTURE diffractometer equipped with a PHOTON 100 CMOS bidimensional detector using a high brilliance  $I\mu$ S microfocus X-ray Mo Ka monochromatized radiation ( $\lambda = 0.71073$  Å). With the aid of Olex2, the structures were solved with the ShelXT structure solution program using Intrinsic Phasing and refined with the ShelXL refinement package using Least Squares minimization. SQUEEZE tool of PLATON was applied to **2**, due to large disordered solvent in the structures. SQUEEZE removed the contributions of some 2556 electrons from the unit-cell contents. Further details about of the crystal structure determinations may be obtained free of charge via the Internet at <https://www.ccdc.cam.ac.uk/> CCDC 2192159 and 2192160. Crystallographic data for single-crystal X-ray diffraction studies are summarized in Table S1.

## Isothermal Titration Calorimetry (ITC)

Isothermal titration calorimetry (ITC) measurements were carried out at 293K using an ITC200 microcalorimeter (MicroCal, LLC, Northampton, MA).  $\{\text{MnMo}_9\}$  0.25 mM in the sample cell was titrated with 5 mM CD (the first 0.2  $\mu\text{L}$  injection was followed by 14 injections of 2  $\mu\text{L}$  with 20 s duration at 150 s time intervals). CD in the syringe was titrated into the identical buffer solution in the sample cell without  $\{\text{MnMo}_9\}$  were used as a control to obtain the dilution heat. Origin (version 7.0) software was used for data analysis. The area of each injection peak was automatically integrated. A binding isotherm curve was obtained by plotting the total heat per injection ( $\text{kcal mol}^{-1}$  of injectant) as a function of the molar ratio of CD to  $\{\text{MnMo}_9\}$ .

## Circular dichroism (CD)

CD spectra were recorded on a MOS-500 CD spectrometer (Bio-Logic Science Instruments, France) using a 5 mm path length quartz cuvette. The scanning speed was set to 200 nm/min, and the response time was 0.5 s.

Solid-state CD spectroscopy: Solid-state CD spectra were recorded by using a MOS-500 CD spectrometer (Bio-Logic Science Instruments, France), The spectra shown in Figure SX were obtained for selected single crystals of compound **1** and compound **2** (see Experimental Section), which had been very carefully ground (to minimize dispersion effects and concentration variations) together with KBr, and then pressed into thin, translucent disks. 1 mg sample and 49 mg KBr are fully ground and mixed evenly, and then put into a  $\text{Ø}13$  mm compression die. Press it for 10 min under 15 MPa to form it, and a transparent circular sheet with a mass fraction of 1/50 is obtained.



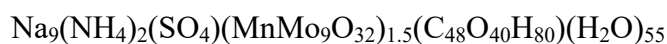
## S3. Synthesis and Experimental Section

### The synthesis of 1:



In a 10 ml beaker, 0.08235 g (0.05 mmol) of  $(\text{NH}_4)_6[\text{MnMo}_9\text{O}_{32}] \cdot 8\text{H}_2\text{O}$  was dissolved in 6 ml of saturated sodium sulfate solution, then 0.05594 g (0.05 mmol) of  $\beta$ -CD was added successively upon stirring at room temperature, after that was heat at 60 °C for 30 min. The clear orange solution was allowed to evaporate in an open vial at room temperature. The block-shaped orange crystals of **1** started to appear after five days, which was collected by filtration and air-dried. Yield: 30.1 % based on  $(\text{NH}_4)_6[\text{MnMo}_9\text{O}_{32}] \cdot 8\text{H}_2\text{O}$ . Elemental analysis: calculated: C, 16.20%; H, 3.43%; N, 2.25%; S, 1.03%, found: C, 15.92%; H, 3.16%; N, 1.52%; S, 0.84%. EDS: Na: 21.94; Mn: 8.23; Mo: 69.84. TGA (Figure S9) reveals a water weight loss of about 9.7% from RT to 143.7°C (the calculated weight loss of 17 H<sub>2</sub>O is 9.8%)

### The synthesis of 2:



In a 10 ml beaker, 0.1235 g (0.075 mmol) of  $(\text{NH}_4)_6[\text{MnMo}_9\text{O}_{32}] \cdot 8\text{H}_2\text{O}$  was dissolved in 6 ml of saturated sodium sulfate solution, then 0.0648 g (0.05 mmol) of  $\gamma$ -CD was added successively upon stirring at room temperature, after that was heat at 60 °C for 30 min. The clear orange solution was allowed to evaporate in an open vial at room temperature. The block-shaped orange crystals of **2** started to appear after five days, which was collected by filtration and air-dried. Yield: 37.2 % based on  $(\text{NH}_4)_6[\text{MnMo}_9\text{O}_{32}] \cdot 8\text{H}_2\text{O}$ . Elemental analysis: calculated: C, 13.45%; H, 5.70%; N, 0.33%; S, 0.75%, found: C, 13.47%; H, 4.91%; N, 0.31%; S, 0.70%. EDS: Na: 38.83; Mn: 7.22; Mo: 53.95. TGA (Figure S10) reveals a water weight loss of about 20.4% from RT to 229°C (the calculated weight loss of 55 H<sub>2</sub>O is 21.5%)

## S4. Crystal data and structure refinement

**Table S1:** Crystal data and structure refinement for **1** and **2**.

Identification code	<b>1</b> (CCDC 2192159)	<b>2</b> (CCDC 2192160)
Empirical formula	C <sub>42</sub> H <sub>49</sub> Mn <sub>1</sub> Mo <sub>9</sub> Na <sub>3</sub> O <sub>78</sub>	C <sub>96</sub> H <sub>112</sub> Mn <sub>3</sub> Mo <sub>27</sub> Na <sub>5</sub> O <sub>18</sub> 1
Formula weight	2790.33	7032.00
Temperature/K	160	160
Crystal system	orthorhombic	orthorhombic
Space group	<i>P</i> 2 <sub>1</sub> 2 <sub>1</sub> 2 <sub>1</sub>	<i>C</i> 222 <sub>1</sub>
<i>a</i> /Å	14.457(5)	19.361(3)
<i>b</i> /Å	24.213(14)	37.863(6)
<i>c</i> /Å	27.46(2)	35.710(6)
$\alpha$ /°	90	90
$\beta$ /°	90	90
$\gamma$ /°	90	90
Volume/Å <sup>3</sup>	9612(10)	26177(7)
<i>Z</i>	4	4
$\rho_{\text{calc}}$ /cm <sup>3</sup>	1.928	1.784
$\mu$ /mm <sup>-1</sup>	1.391	1.493
F(000)	5446	13600
Radiation	MoK $\alpha$ ( $\lambda$ = 0.71073)	MoK $\alpha$ ( $\lambda$ = 0.71073)
2 $\Theta$ range for data collection/°	4.388 to 54.856	4.36 to 55.12
Index ranges	-17 $\leq$ <i>h</i> $\leq$ 18, -31 $\leq$ <i>k</i> $\leq$ 31, -35 $\leq$ <i>l</i> $\leq$ 35	-23 $\leq$ <i>h</i> $\leq$ 25, -47 $\leq$ <i>k</i> $\leq$ 49, -46 $\leq$ <i>l</i> $\leq$ 46
Reflections collected	77752	96965
Independent reflections	21773 [ <i>R</i> <sub>int</sub> = 0.0377, <i>R</i> <sub>sigma</sub> = 0.0384]	29920 [ <i>R</i> <sub>int</sub> = 0.0485, <i>R</i> <sub>sigma</sub> = 0.0577]
Data/restraints/parameters	21773/2166/1243	29920/2657/1856
Goodness-of-fit on <i>F</i> <sup>2</sup>	1.061	1.037
Final <i>R</i> indexes [ <i>I</i> $\geq$ 2 $\sigma$ ( <i>I</i> )]	<i>R</i> <sub>1</sub> = 0.0535, <i>wR</i> <sub>2</sub> = 0.1611	<i>R</i> <sub>1</sub> = 0.0790, <i>wR</i> <sub>2</sub> = 0.2292
Final <i>R</i> indexes [all data]	<i>R</i> <sub>1</sub> = 0.0575, <i>wR</i> <sub>2</sub> = 0.1676	<i>R</i> <sub>1</sub> = 0.1003, <i>wR</i> <sub>2</sub> = 0.2501
Largest diff. peak/hole / e Å <sup>-3</sup>	2.60/-1.23	2.83/-1.54
Flack parameter	0.017(8)	0.073(11)

## S5. Additional structural figures

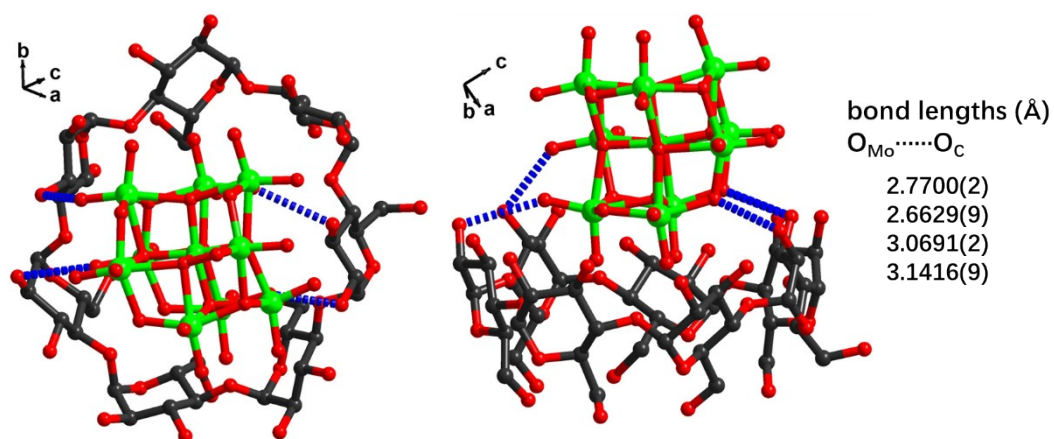


Figure S1. Top and side views of hydrogen bonds (blue dotted line) of  $O_{Mo} - O_C$  between  $\{MnMo_9\}$  Keggin unit and  $\beta$ -CD in **1**. Color codes: Mn and Mo green; C black; O red; hydrogen atoms are omitted for clarity.

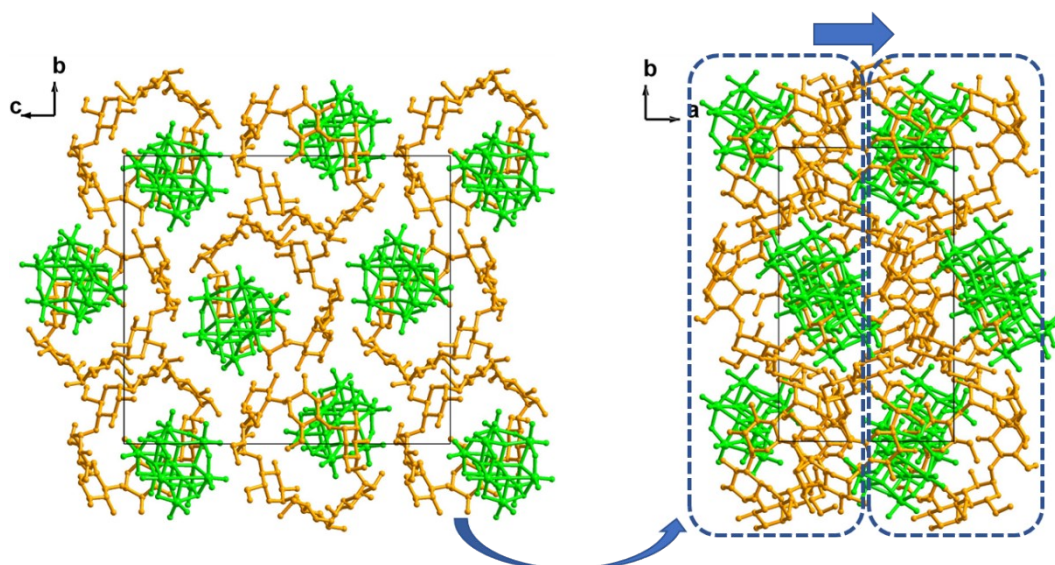


Figure S2. Ball-stick stacking representation of the crystal structure of **1**. The  $\{MnMo_9\}@ \beta$ -CD as the basic repeating unit interweave with the adjacent units as the staggered stack to two-dimensional (2D) layers on the  $bc$ -plane. The layers extend parallelly along the  $a$ -axis to give rise to 3D framework. Color code:  $\beta$ -CD, yellow;  $\{MnMo_9\}$ , green.

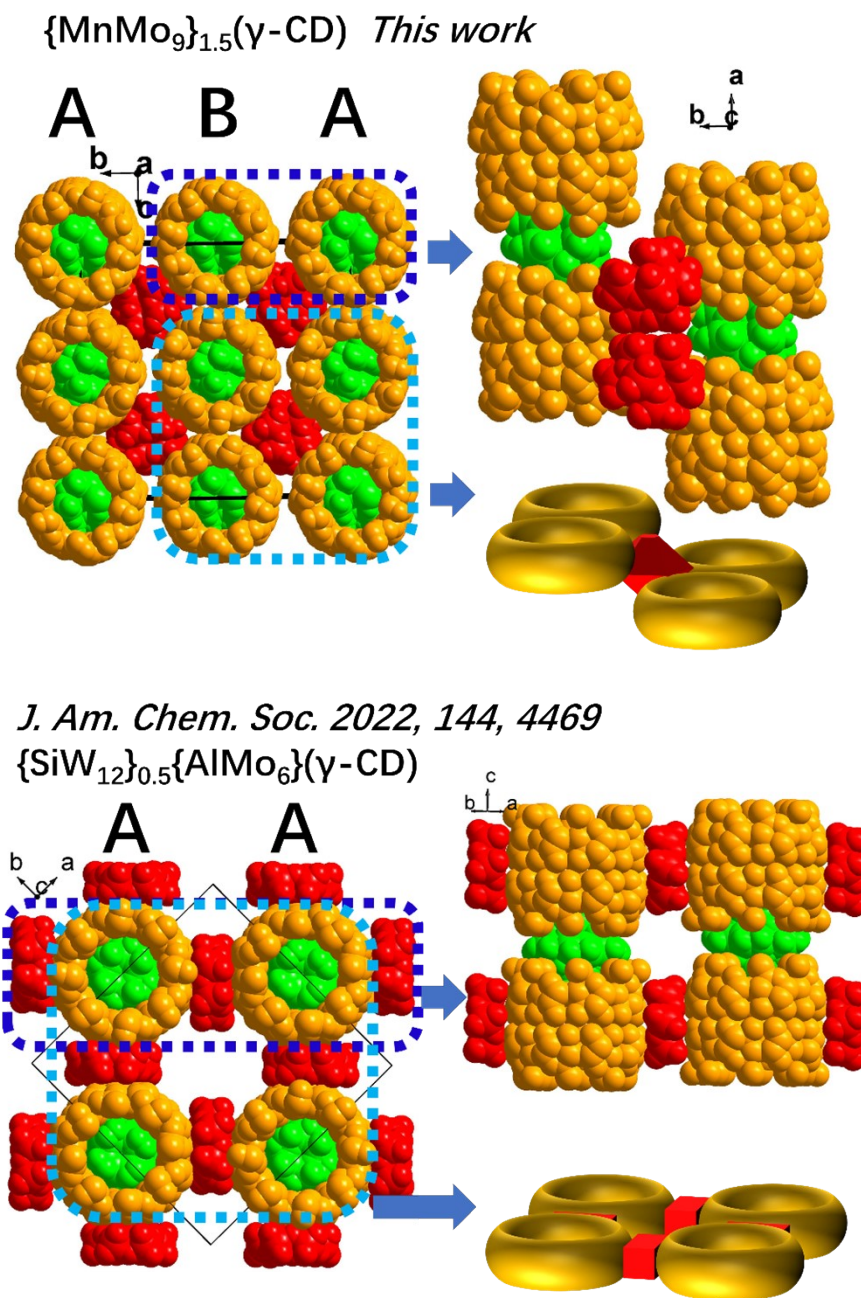


Figure S3. Comparison of  $\{\text{MnMo}_9\}_{1.5}(\gamma\text{-CD})$  with the structure  $\{\text{SiW}_{12}\}_{0.5}\{\text{AlMo}_6\}(\gamma\text{-CD})$  reported by Falaise and coworker (*J. Am. Chem. Soc.* 2022, 144, 4469). The hybrid POM/CD rods are similar and are built from alternating cyclodextrin dimers and Keggin-type POMs or Waugh-type POMs. In both structures, the POMs anion interacts with the primary face of the CD. The main difference is the arrangements of hybrid POM/CD rods due to the presence of the  $\{\text{MnMo}_9\}$  unit that act as a spacer for the hybrid rods, forming a staggered overlap with a  $\{\text{MnMo}_9\}$  offset distance in  $\{\text{MnMo}_9\}_{1.5}(\gamma\text{-CD})$ . Furthermore, one  $\{\text{MnMo}_9\}$  decorates four  $(\gamma\text{-CD})_2$  dimers to lead to a dense phase, while the presence of  $\{\text{AlMo}_6\}$  linked two  $(\gamma\text{-CD})_2$  dimers provides the formation of large voids in  $\{\text{SiW}_{12}\}_{0.5}\{\text{AlMo}_6\}(\gamma\text{-CD})$ .



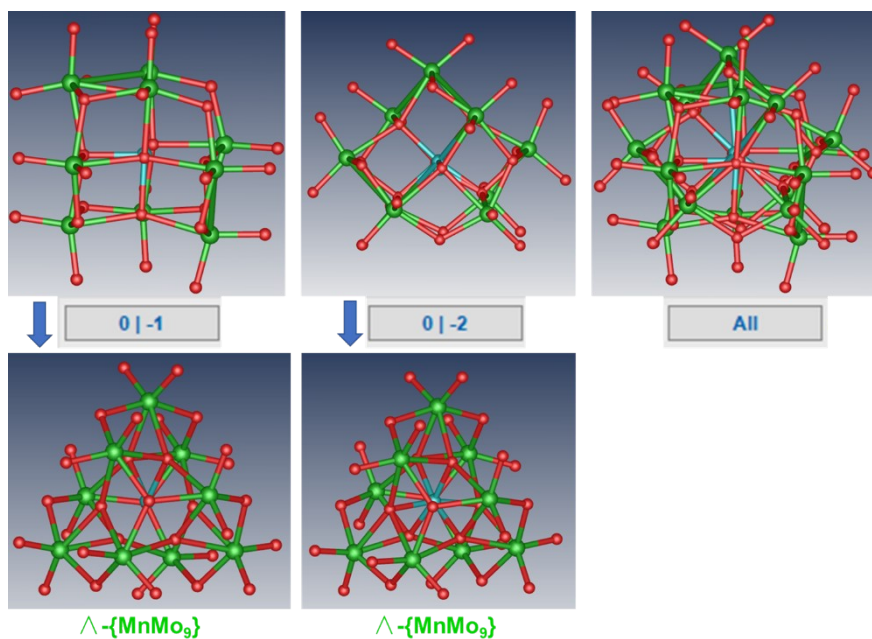


Figure S4. The disordered POM with two positions shown in the OLEX2 interface. The  $\gamma$ -CD and another ordered POM are ignored for clarity.

The single crystal X-ray diffraction data of the compound 2 shows that it contains one perfectly ordered POM (anticlockwise enantiomer) and another one which is highly disordered (occupancy of about 25%). The disordered POM was refined with two positions as shown in Figure S4. Both part 1 and 2 of POM show the anticlockwise enantiomer. The reliable structural model is certificated by the final r-values ( $R1 = 0.0792$ ).

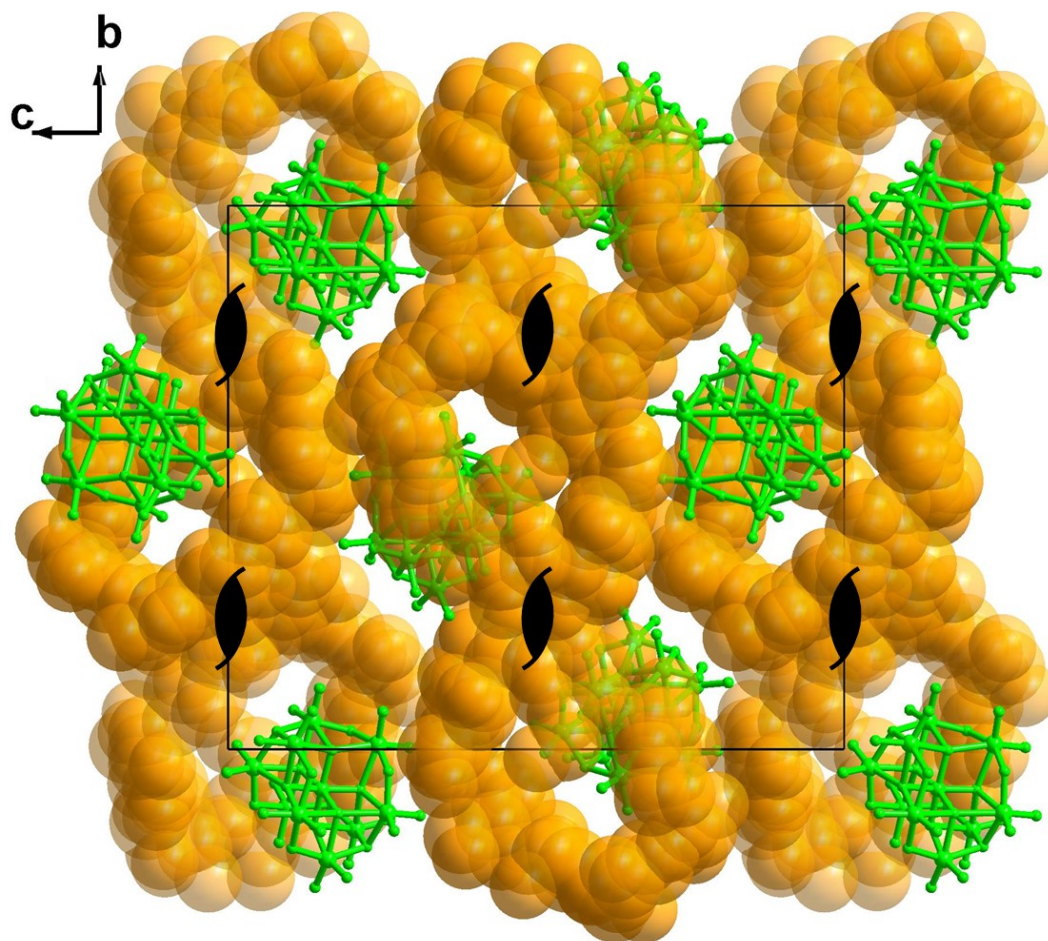


Figure S5. Solid-state superstructure of the  $\Lambda$ - $\{\text{MnMo}_9\}$  and  $\beta$ -CD obtained by X-ray diffraction displaying a space-fill and ball-stick representation held around an enantiomorphous  $2_1$  screw axis. Color code:  $\beta$ -CD, yellow;  $\{\text{MnMo}_9\}$ , green.

## S6. $^1\text{H}$ NMR spectra

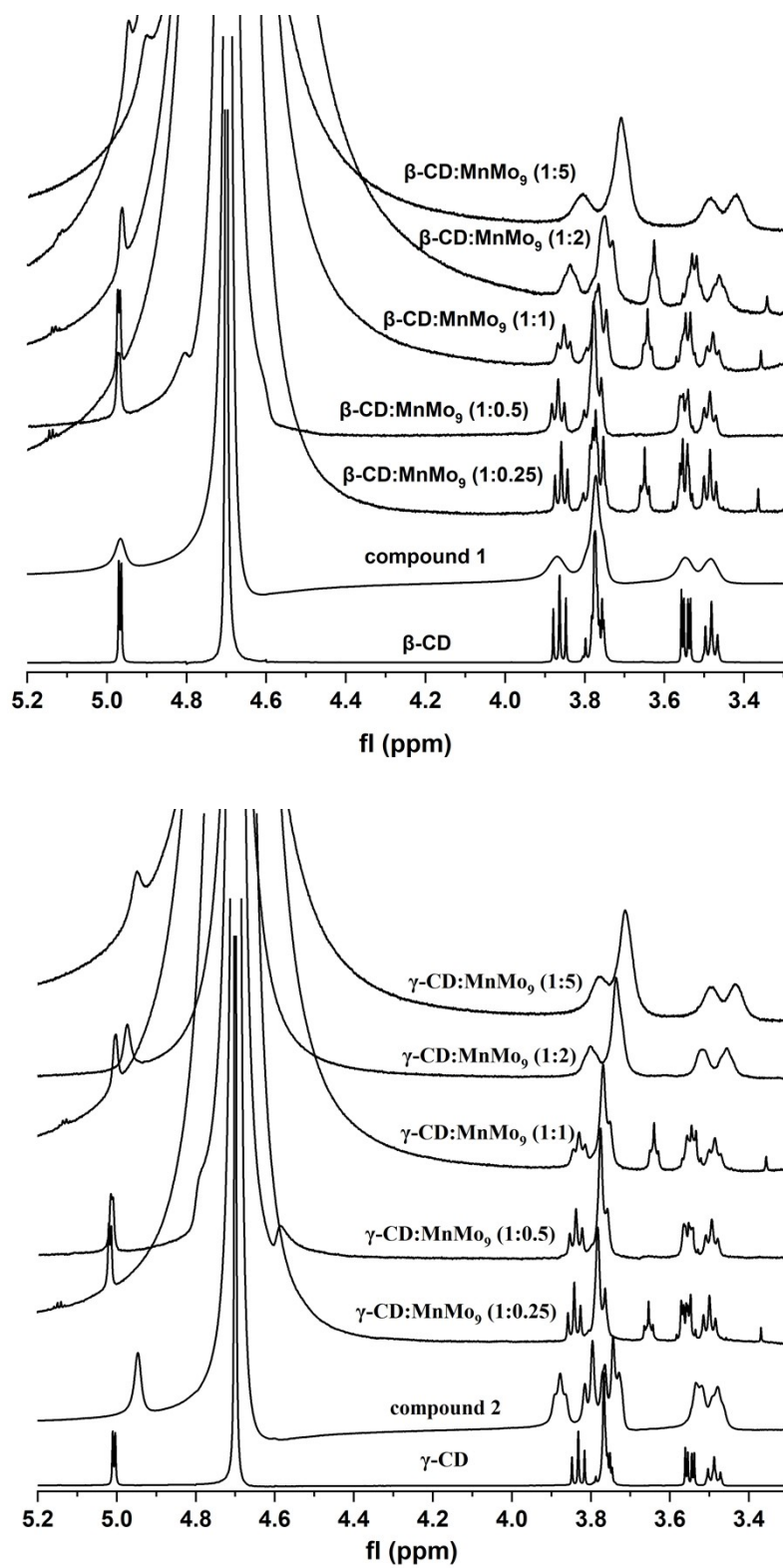


Figure S6.  $^1\text{H}$  NMR spectra of aqueous  $\beta\text{-CD}$  (1 mM) and  $\gamma\text{-CD}$  (1 mM) solution with  $\{\text{MnMo}_9\}$ .

Table S2. The summary of chemical shifts of two cyclodextrins and their mixtures with  $\text{MnMo}_9$  from Figure S6.

	H1 (ppm)	H2 (ppm)	H3 (ppm)	H4 (ppm)	H5 (ppm)	H6 (ppm)
$\beta$ -CD	4.97	3.56	3.86	3.48	3.76	3.77
$\Delta\delta$ $\beta$ -CD@ $\{\text{MnMo}_9\}$	0.01	0.01	0.00	0.00	-0.01	0.00
$\Delta\delta$ $\beta$ -CD : $\{\text{MnMo}_9\}$ (1:0.25)	0.00	0.01	0.00	0.00	0.01	0.00
$\Delta\delta$ $\beta$ -CD : $\{\text{MnMo}_9\}$ (1:0.5)	0.00	0.02	-0.01	0.00	0.00	-0.01
$\Delta\delta$ $\beta$ -CD : $\{\text{MnMo}_9\}$ (1:1)	0.01	0.03	0.01	0.00	0.02	0.01
$\Delta\delta$ $\beta$ -CD : $\{\text{MnMo}_9\}$ (1:2)	0.03	0.03	0.02	0.02	0.03	0.02
$\Delta\delta$ $\beta$ -CD : $\{\text{MnMo}_9\}$ (1:5)	0.07	0.07	0.05	0.05	0.05	0.06
$\gamma$ -CD	5.01	3.61	3.83	3.49	3.75	3.77
$\Delta\delta$ $\gamma$ -CD@ $\text{MnMo}_9$	0.06	0.08	-0.05	0.01	0.01	-0.02
$\Delta\delta$ $\gamma$ -CD : $\{\text{MnMo}_9\}$ (1:0.25)	0.00	0.07	-0.01	0.00	-0.01	-0.01
$\Delta\delta$ $\gamma$ -CD : $\{\text{MnMo}_9\}$ (1:0.5)	0.00	0.05	-0.01	0.00	-0.01	-0.01
$\Delta\delta$ $\gamma$ -CD : $\{\text{MnMo}_9\}$ (1:1)	0.01	0.07	0.00	0.00	0.00	0.00
$\Delta\delta$ $\gamma$ -CD : $\{\text{MnMo}_9\}$ (1:2)	0.04	0.09	0.03	0.04	0.01	0.03
$\Delta\delta$ $\gamma$ -CD : $\{\text{MnMo}_9\}$ (1:5)	0.06	0.11	0.05	0.05	0.04	0.06

The NMR signatures of CDs are almost not affected by the presence of  $\{\text{MnMo}_9\}$ , meaning there is no or weak interaction between the macrocycle and the POM.

## S7. Fourier Transform Infrared Spectroscopy

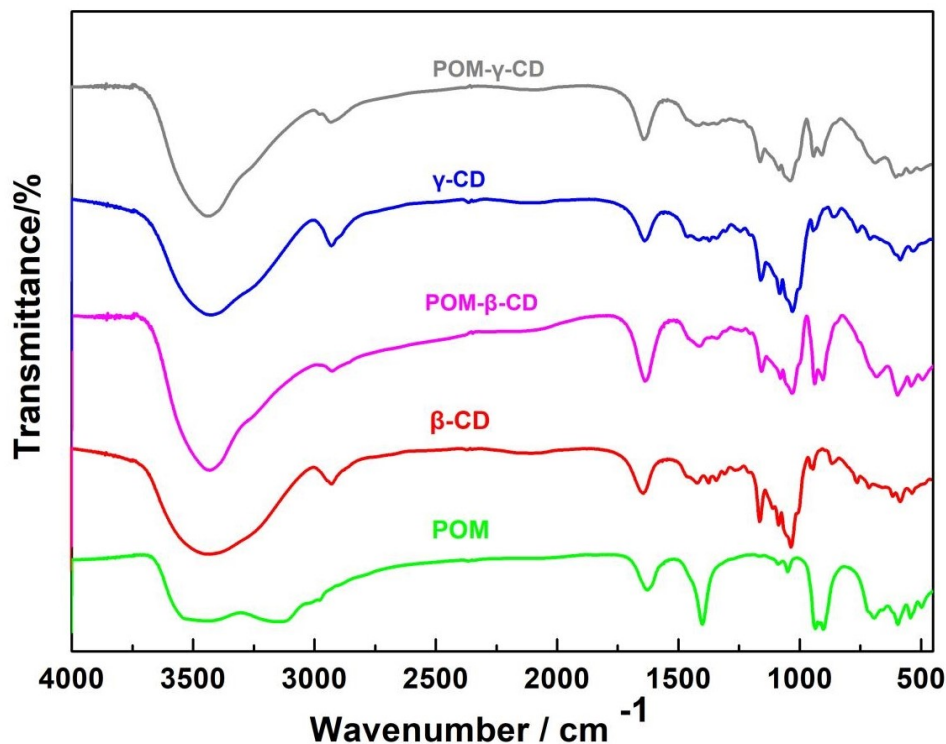


Figure S7. FT-IR spectra of POM, CD, compound 1 and compound 2.

The infrared spectrum of  $(\text{NH}_4)_6[\text{MnMo}_9\text{O}_{32}] \cdot 8\text{H}_2\text{O}$  shows that it is between 400 ~ 1000  $\text{cm}^{-1}$ . In the range, the vibration peaks 940  $\text{cm}^{-1}$  and 900  $\text{cm}^{-1}$  are the stretching vibration peaks of Mo-O. The reason for the splitting of vibration peaks is that the chemical environment of Mo-O double bond is different, resulting in different bond lengths of Mo=O; The vibration peaks 690  $\text{cm}^{-1}$ , 593  $\text{cm}^{-1}$  and 540  $\text{cm}^{-1}$  are produced by the bending vibration of Mo-O-Mo. The vibration peak splitting is due to the difference in the chemical environment between some  $\text{MoO}_6$  octahedrons and  $\text{MoO}_6$  octahedrons, which makes the length of Mo-O-Mo bond caused by different; The vibration peak 500  $\text{cm}^{-1}$  is the peak produced by the bending vibration of Mn-O-Mo; The Mn-O stretching vibration peak is covered by the bending vibration peak of Mo-O-Mo. 3159  $\text{cm}^{-1}$  (N-H), 1400  $\text{cm}^{-1}$  (H-N-H), 3420  $\text{cm}^{-1}$  (O-H), 1627  $\text{cm}^{-1}$  (O-H-O), 1100  $\text{cm}^{-1}$  (S-O) are the vibration absorption peaks of  $\text{NH}_4^+$ ,  $\text{SO}_4^{2-}$  and  $\text{H}_2\text{O}$ .

On the other hand, the cyclodextrin has strong absorption peak of O-H bonds located at around 3440  $\text{cm}^{-1}$ . The band centered at around 2930  $\text{cm}^{-1}$  belongs to the asymmetrical stretching vibration of C-H bonds. While the band at around 1640  $\text{cm}^{-1}$  originates from the C-C stretching of polysaccharides. The peaks occur in the region from 1470 to 1180  $\text{cm}^{-1}$  correspond to the C-H bending vibrations while the band located between 1150~1000  $\text{cm}^{-1}$  is characteristic of the symmetrical stretching of glycosidic C-O-C and C-O bonds in polysaccharides.

## S8. Powder X-ray diffraction (PXRD)

The Powder X-ray diffraction (PXRD) patterns for **1** and **2** can be compared with the simulated pattern obtained from the X-ray single-crystal diffraction analysis. Their peak positions are in good agreement with each other, indicating the phase purity of the product. The differences in intensity may be due to the preferred orientation of the powder sample.

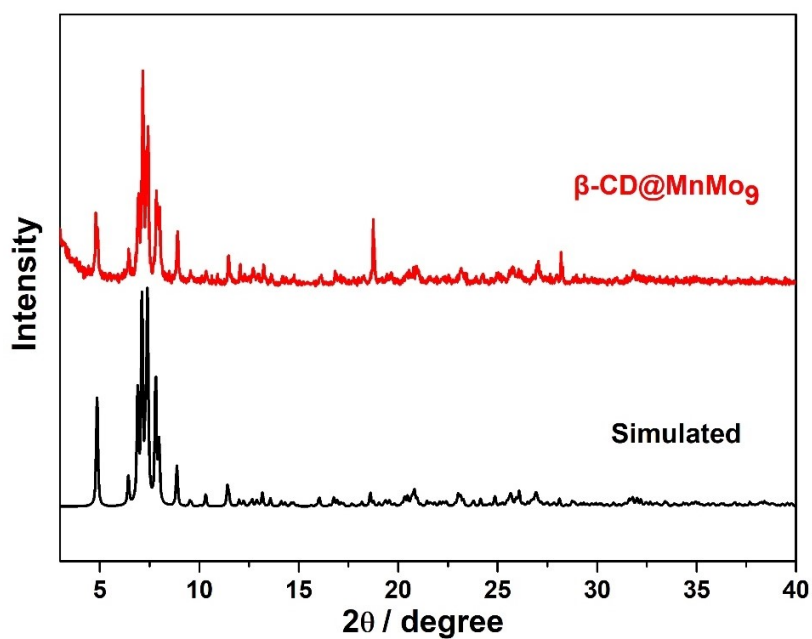


Figure S8. PXRD pattern of **1**.

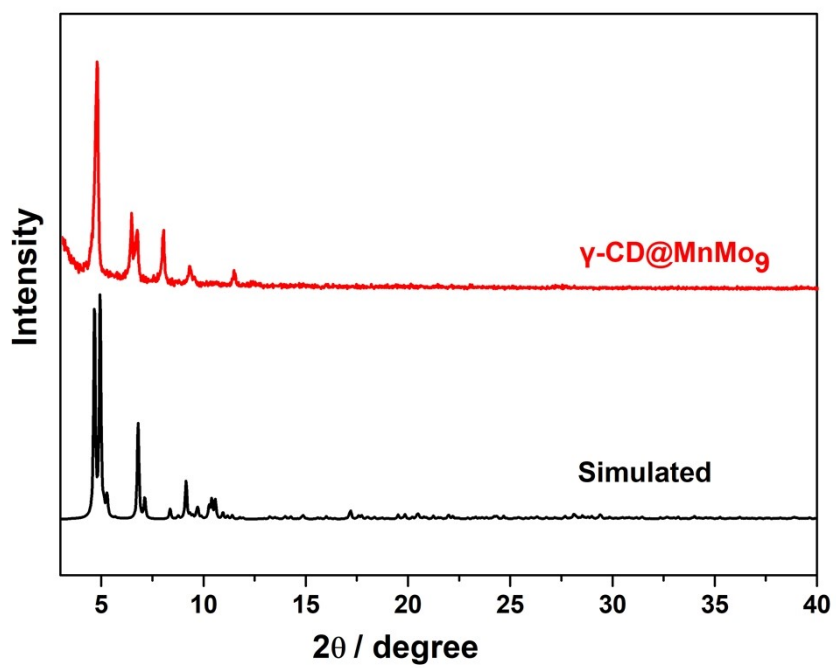


Figure S9. PXRD pattern of **2**.

## S9. Thermogravimetric analyses (TGA)

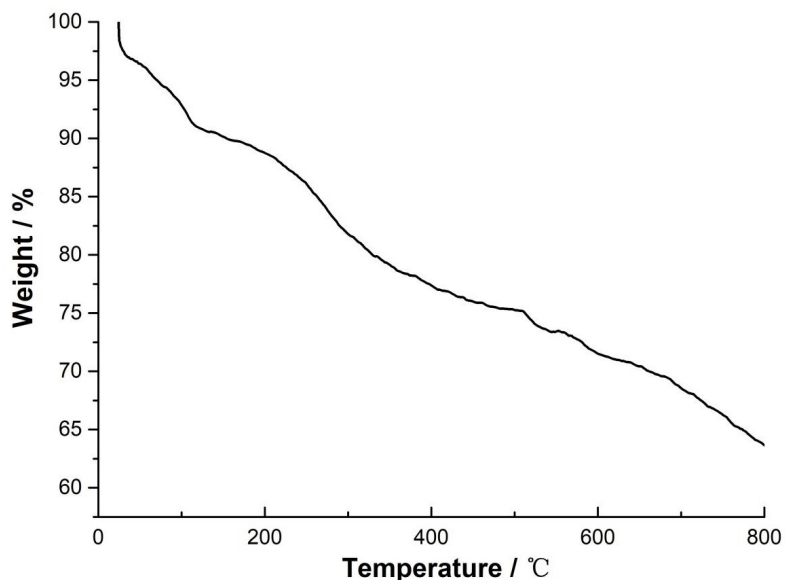


Figure S10. Thermogravimetric analysis trace of **1**.

The thermogravimetric test with heating rate of 10 °C/min in nitrogen atmosphere shows that the weight loss in the first stage (30 °C-143.7 °C) is about 9.70%, mainly due to the loss of water molecules in the lattice.

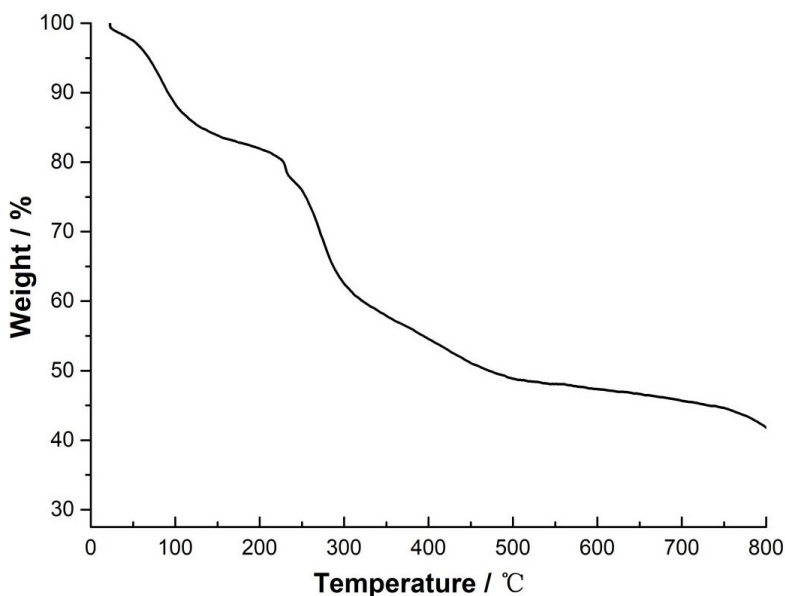


Figure S11. Thermogravimetric analysis trace of **2**.

The thermogravimetric test with heating rate of 10 °C/min in nitrogen atmosphere shows that the weight loss in the first stage (50 °C-229 °C) is about 20.4%, mainly due to the loss of water molecules in the lattice.



# S10. Energy dispersive spectrum analysis (EDS)

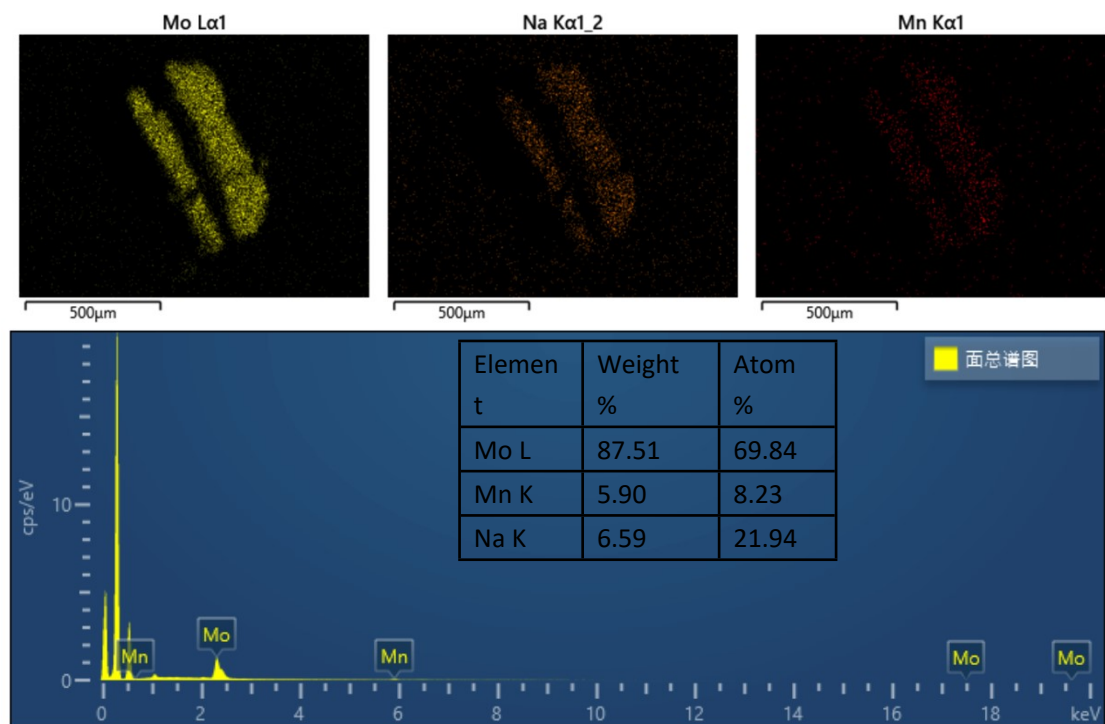


Figure S12. Energy-dispersive X-ray spectroscopy of 1.

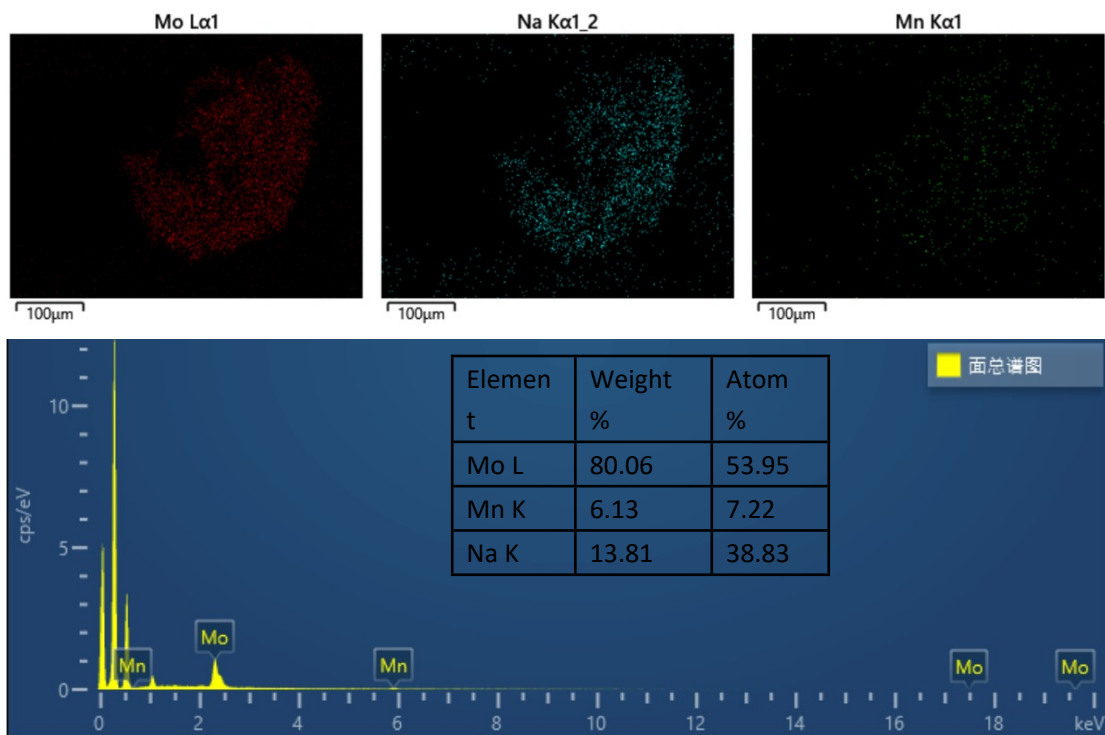




Figure S13. Energy-dispersive X-ray spectroscopy of 2.

## S11. Enantiomers of {MnMo<sub>9</sub>} in 1 and 2

Table 3. SCXRD analysis of crystals picked in the one beaker for one-time synthesis.

Analysis object of <b>1</b>	Number	Space group	R <sub>1</sub>	Flack	Enantiomer
	1	<i>P2<sub>1</sub>2<sub>1</sub>2<sub>1</sub></i>	0.0524	0.018(8)	Λ-{MnMo <sub>9</sub> }
	2	<i>P2<sub>1</sub>2<sub>1</sub>2<sub>1</sub></i>	0.0742	0.044(7)	Λ-{MnMo <sub>9</sub> }
	3	<i>P2<sub>1</sub>2<sub>1</sub>2<sub>1</sub></i>	0.0792	0.085(7)	Λ-{MnMo <sub>9</sub> }
	4	<i>P2<sub>1</sub>2<sub>1</sub>2<sub>1</sub></i>	0.0772	0.061(9)	Λ-{MnMo <sub>9</sub> }
Analysis object of <b>2</b>	Number	Space group	R <sub>1</sub>	Flack	Enantiomer
	1	<i>C222<sub>1</sub></i>	0.0832	0.038(11)	Λ-{MnMo <sub>9</sub> }
	2	<i>C222<sub>1</sub></i>	0.0748	0.046(11)	Λ-{MnMo <sub>9</sub> }
	3	<i>C222<sub>1</sub></i>	0.0659	0.020(8)	Λ-{MnMo <sub>9</sub> }
	4	<i>C222<sub>1</sub></i>	0.0677	0.005(9)	Λ-{MnMo <sub>9</sub> }

## S12. Isothermal Titration Calorimetry (ITC)

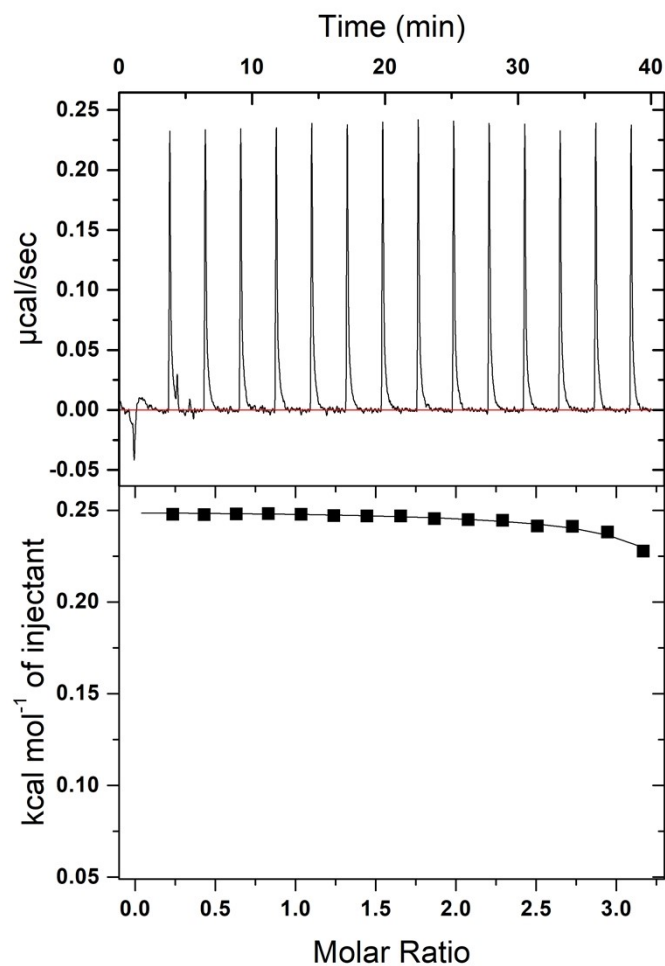


Figure S14. ITC thermograms (upper part) and isotherms (lower part) for the system  $\beta$ -CD/{MnMo<sub>9</sub>}.

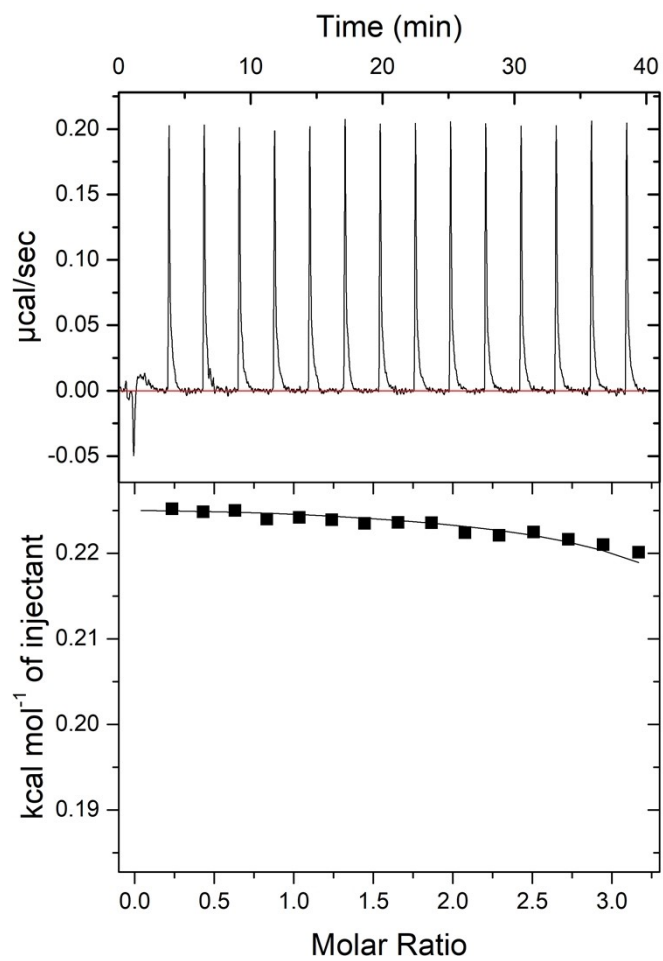


Figure S15. ITC thermograms (upper part) and isotherms (lower part) for the system  $\gamma$ -CD/{MnMo<sub>9</sub>}.

## S13. Circular dichroism (CD)

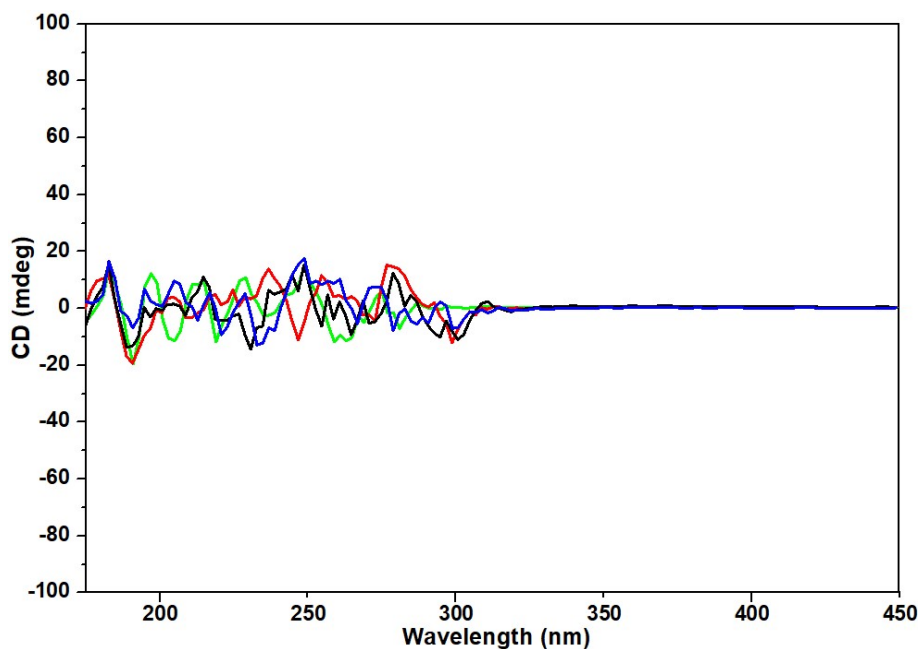


Figure S16. The CD spectra of compound 1 (black,  $c = 1.0 \times 10^{-3}$  M) and compounds 2 (blue,  $c = 1.0 \times 10^{-3}$  M) and (NH<sub>4</sub>)<sub>6</sub>MnMo<sub>9</sub>O<sub>32</sub> (red,  $c = 1.0 \times 10^{-3}$  M) and (NH<sub>4</sub>)<sub>6</sub>Mo<sub>7</sub>O<sub>24</sub> (green,  $c = 1.0 \times 10^{-3}$  M) in H<sub>2</sub>O solution.

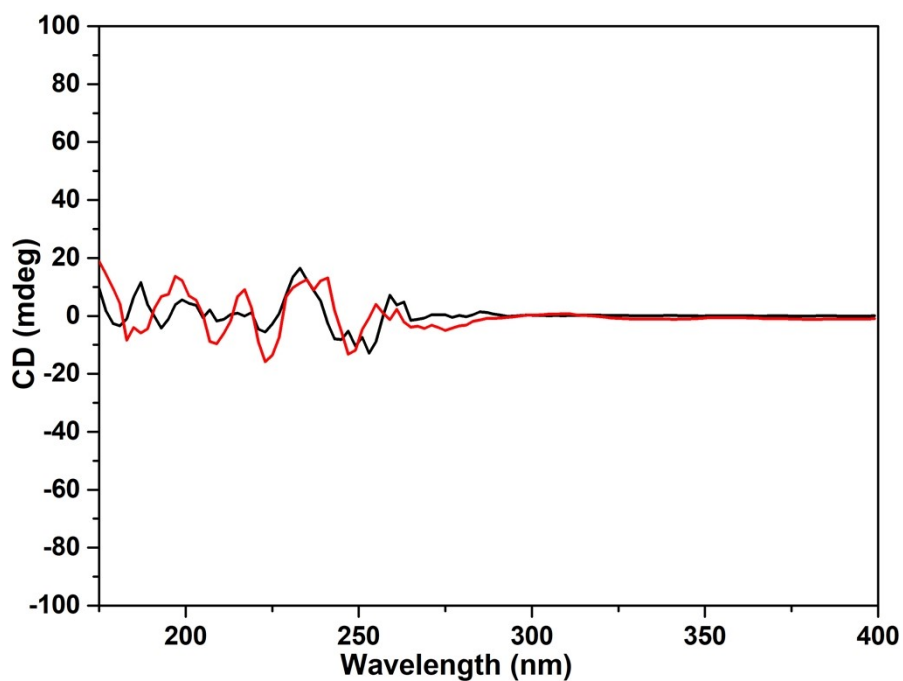
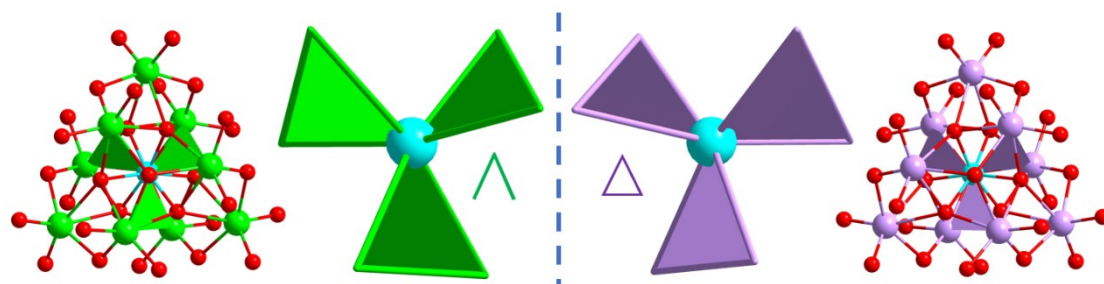


Figure S17. The CD spectra of (NH<sub>4</sub>)<sub>6</sub>MnMo<sub>9</sub>O<sub>32</sub> ( $c = 0.25 \times 10^{-3}$  M) with 4-fold excess of  $\beta$ -CD (black) and  $\gamma$ -CD (red).

## S14. Computational details

Calculations were performed by using the B3LYP/LanL2DZ method as implemented in Gaussian 03 program. We only considered the framework containing Mn, Mo, and O atoms which are shown in the Figure S18 (up panel).



	jacs073153w	Compound 1	Compound 2
$\Lambda$ -{MnMo <sub>9</sub> }	0	-4.0 kcal/mol	13.13 kcal/mol
$\Delta$ -{MnMo <sub>9</sub> }	3.72 kcal/mol		

Figure S18. Relative energy and structure of  $\Lambda$  and  $\Delta$ {MnMo<sub>9</sub>}. (jacs073153w :  $\Lambda$ -{MnMo<sub>9</sub>} and  $\Delta$ -{MnMo<sub>9</sub>} enantiomer from the reference of [13b]. *J. Am. Chem. Soc.*, 2007, 129, 10066)